scientific reports

Check for updates

OPEN

Age-related decline in behavior and reproductive health in male mice

Larissa Araújo Stábile[1], Camilla Mota Mendes[1], Thais Rose dos Santos Hamilton[1,3], Marcelo Demarchi Goissis[1], Álvaro de Miranda Alves[1], Marcílio Nichi[1], Heriberto Barbosa-Moyano[1], Mariana de Souza Aranha Garcia-Gomes[2], Claudia Madalena Cabrera Mori[2], José Antônio Visintin[1] & Mayra Elena Ortiz D'Ávila Assumpção[1]✉

Research on reproductive advanced age has predominantly focused on women due to their biological clock. The impact of paternal senescence on fertility and offspring is still poorly understood. In this study, we characterized the effects of aging on sexual behavior and reproductive characteristics using male mice aged 4 months as a control, compared to mice aged 19 and 24 months. In the first experiment, we observed that reproductive interest and locomotor activity were reduced in older males, accompanied by reduced serum testosterone levels and testicular weight. We observed increased sperm morphological anomalies, protamine deficiency, and reduced sperm capacitation in aging mice. Aging also influenced cleavage, blastocyst and in vitro embryo development rates; embryo kinetics, and initial cell differentiation. In the second experiment, aging promoted smaller, lighter fetuses and a lower fetal weight ratio. In conclusion, an increased age impaired sexual behavior, sperm function, and embryo and fetal development.

In the last decades, there has been a significant demographic change in the parenting age. Between 1993 and 2003, there was a shift in paternal age trends, with approximately 38% increase in births from fathers aged from 35 to 54 years (99,500 to 136,500), while births from fathers under 30 years declined by approximately 33% (285,00 to 192,00)[1]. In the United States, the paternal age average was 32.1 years in 2022, and as paternal age increases, maternal partners tend to be older as well, with most mothers between the ages of 31 to 40 years and 41 to 50 years[2]. This also happens in Europe; many fathers were over 33 years old, and mothers had an average age of 30.2 to 31.5 years[3,4].

This shift reflects social changes, such as delayed fatherhood due to career advancements, economic stability, and increased access to assisted reproductive technologies[5,6]. Historically, when considering age and fertility, attention has focused on women, and it was believed that men could father offspring indefinitely[7]. Although this is partially true, it is now widely recognized that delaying fatherhood raises concerns about on impact on male reproductive health, pregnancy outcomes, and offspring well-being.

One of the hallmarks of male aging is the decline in sexual behavior, including reduced libido and erectile dysfunction[8]. Feldman et al.[9] reported that the probability of severe erectile dysfunction triples in men aged 40 to 70 years. Additionally, sexual activity decreases with age, from an average of 6.5 sexual encounters per month at age 40 to 1–2 encounters after age 50. Similar trends have been observed in mice, where males aged 18 to 27 months exhibit reduced mating frequency and reproductive efficiency[10,11].

These changes are strongly influenced by age-related hormonal decline, particularly in testosterone levels, which are fundamental for spermatogenesis and fertility. Harman et al.[12] observed that, after the age of 30, testosterone levels in men decline by 0.4% to 2% per year. This pattern is also observed in various mouse strains, including C57BL/6[13], CD1[14], SAMP8[15] and CBA/Ca[16].

These hormonal changes may still be secondary to alterations in the testicular microenvironment. Neaves et al.[17] reported that men aged 50–76 experience a 50% reduction in Leydig cells, compromising testosterone production and spermatogonia development. Additionally, Sertoli cell numbers decrease after the fifties in humans, reducing the supportive environment required for spermatogenesis.

[1]Department of Animal Reproduction, School of Veterinary Medicine and Animal Science, University of Sao Paulo, Sao Paulo 05508 270, Brazil. [2]Department of Pathology School of Veterinary Medicine and Animal Science, University of Sao Paulo, Sao Paulo 05508 270, Brazil. [3]Department of Animal Morphology and Physiology, School of Agriculture and Veterinary Science, Sao Paulo State University, Jaboticabal 14884 900, Brazil. ✉email: meoaa@usp.br

Spermatogenesis is a highly regulated process that depends on a stable testicular microenvironment and hormonal balance. Three key elements are required for successful sperm production: (1) maintenance of normal cell cycle progression to sustain the spermatogonial population, (2) continuous meiotic division to generate haploid spermatids and (3) effective spermiogenesis to ensure structural integrity and functional maturation of spermatozoa[18].

However, aging disrupts these processes, affected physically, such as a compromised blood-testis barrier, thinner tunica albuginea, and degenerated seminiferous tubules[19]; through spontaneous mutations[20,21], cellular apoptosis, abnormal metabolism, reduced ability to resist oxidative damage[22], and epigenetic modifications[23]. Leading to increased rates of abnormal sperm morphology, DNA fragmentation, and reduced motility.

Eskenazi et al.[24] demonstrated sperm concentration decrease in men (5% at 30, 10% at 50, and 35% at 80). Kumar et al.[25] observed that men aged between 21 and 28 years had 26.05% of sperm with normal morphology, while men aged between 50 and 60 years had 19.73%, resulting in a 6.32% decrease in the percentage of healthy sperm. Pino et al.[26] reported that men over 50 presented reduced ejaculate volume, sperm concentration, and increased DNA fragmentation, while men over 31 already showed decreased sperm motility. Similarly, Sloter et al.[27] reported an annual decline of 0.8% in total motility and 0.9% in progressive motility.

Age-related sperm alterations extend beyond male fertility, negatively impacting pregnancy outcomes and offspring health. Women with partners aged ≥ 45 years have a 48% increased risk of stillbirth, a 19% higher likelihood of low birth weight, and a 13% increased risk of preterm birth[28]. Additionally, a meta-analysis of 975 studies confirmed that paternal age ≥ 45 years significantly increases the risk of spontaneous miscarriage, with risk rising progressively from age 40 onward[29]. Also, some studies have reported IVF/ICSI success rate[30], chromosomal errors[31] and a decline in placentas[32] weight. Additionally, long-term health repercussions for offspring, such as neurocognitive disorders, have been observed[33–35].

With this evidence, some studies have identified correlations between sperm alterations and offspring health problems. However, many aspects of paternal aging remain unclear. Studies with human subjects face numerous challenges, including ethical concerns, genetic, environmental, and behavioral variability, medical history, and sample size limitations[36]. In contrast, the mouse model offers new insights into aging due to its short lifespan, enabling longevity studies (reviewed by Stábile et al.[10]). Moreover, reproductive changes (reviewed by[11,37–40], have been shown in mice, with high consistency with aging phenotypes observed in humans.

While our previous work[10] demonstrated that male aging negatively affects fertility outcomes, the precise onset and progression of these changes remain unclear. The literature is inconsistent, with studies in mice using a broad range of ages, such as 12, 13, 15, 18, or 24 months, without defining a clear cutoff for the onset of reproductive senescence. To address this gap, we selected 19 month old mice (equivalent to ~ 64 human[41]) as a representative intermediate stage, based on prior observations indicating a functional transition in reproductive behavior at this age. Notably, some males at 18 months already show reduced sexual responsiveness, suggesting that 19 months may mark the lower threshold of reproductive aging. In contrast, 24 month old mice (equivalent to ~ 73 human years[41]) are widely accepted as a model of advanced aging. Comparing these two timepoints allows us to assess whether reproductive decline occurs progressively or becomes more pronounced at later stages.

Therefore, knowing that paternal aging is already associated with reduced serum testosterone levels and abnomal sperm morphology, we hypothesize that aged male (19 and 24 months old) exhibits additional reproductive decline, including reduced psychomotor activity and sexual behavior. Futhermore, even when mating occurs, reproductive success may be impaired due to alterations in sperm fitness, such as impaired protamination and reduced capacitation efficiency, ultimately leading to lower embryo and conceptus development parameters. These combined effects constitute a multifactorial decline in male reproductive capacity with advancing age, extending beyond what is reported in existing literature.

To address these questions, in Experiment 1 we assessed mating attempts (spontaneous social interaction with synchronized females), exploratory activity and anxiety-like behavior (open field), and spatial memory (spontaneous alternation in the T-maze). While the open field and T-maze are not traditional tests of reproductive behavior, they are essential for evaluating the animal's overall functional status. In rodents, general health and behavioral engagement are closely linked to reproductive success. We measured serum testosterone and evaluated sperm morphology, motility patterns, sperm functionality, DNA compaction and fragmentation susceptibility, and capacitation status. We also analyzed in vivo fertility and in vitro embryo development rates, embryonic stage at embryonic day 4.5, and cell allocation after first differentiation. In Experiment 2, we examined conceptus development at 16 days of gestation, including fetuses, placental, and characteristic of the litter size. We concluded that paternal aging negatively affects sexual behavior, sperm fitness, and both embryo and fetal development.

Results

In Experiment 1, males from all three age groups (4, 19, and 24 months) were evaluated for behavioral analyses, sperm parameters, and in vitro embryo development, with the same animals used across all assessments. In Experiment 2, in vivo fetal development was assessed using a separate cohort of males, with comparisons conducted between the 4- and 19-month groups and the 4- and 24-month groups. In both experiments, all animals were evaluated contemporaneously to ensure consistency across age groups. The schematic representation of the experimental design can be seen in Fig. 1.

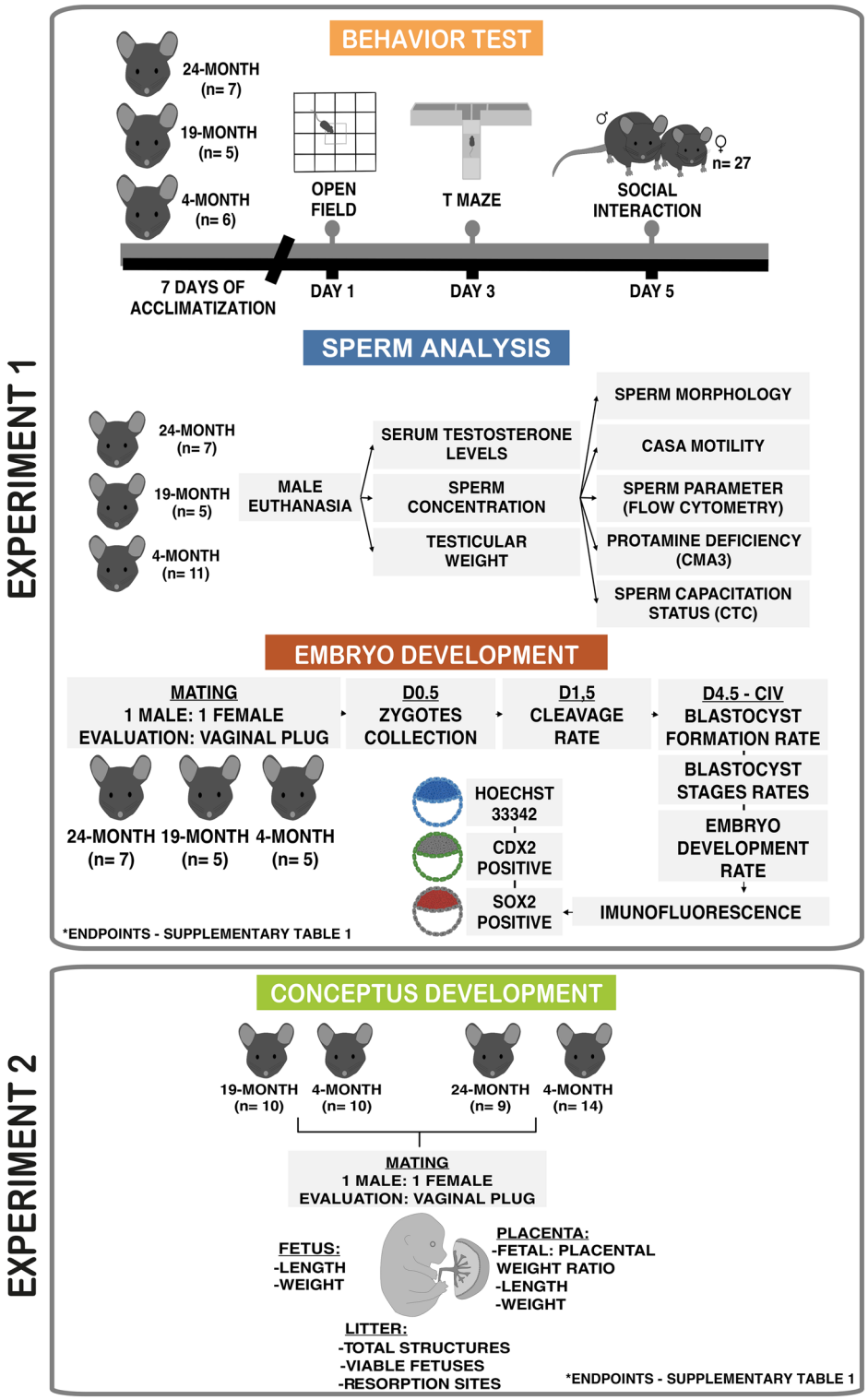


Fig. 1. Experimental design. The experimental design consisted of two contemporary blind experiments involving males aged 4 (control group), 19 and 24 months (experimental groups), and young females (2 to 3 months) for mating. In Experiment 1, the ages of 4, 19, and 24 months were compared, using the same males for behavioral, sperm, and in vitro embryo development analyses. In Experiment 2, in vivo fetal development was evaluated using different males, comparing groups of 4 versus 19 months and 4 versus 24 months, ensuring the contemporaneity of the groups. Endpoints were applied based on predefined criteria, as detailed in the scoring table provided in Supplementary Material 1.

Experiment 1

Behavioral assessments

Aging male mice exhibit reduced locomotor activity on open-field test. We found that the 19- and 24-month aging groups showed a reduced total distance traveled compared to the 4-month group ($p = < 0.0001$; Fig. 2a). The frequencies of entry into the central zone ($p = 0.002$) and peripheral zone ($p = 0.002$) were lower in the 19- and 24-month groups compared to the 4-month group (Fig. 2b). Furthermore, 24-month males showed a reduction in rearing frequency compared to the control group ($p = 0.023$; Fig. 2c). The aging groups spent most of their time in the same place they were initially positioned (center point) compared to the young animals ($p = 0.001$; Fig. 2d). Conversely, movement time at the central point ($p = 0.001$; Fig. 2d) was longer in the 4-month group compared to the 19- and 24-month groups. Aging animals had a lower average speed than young ones ($p = < 0.0001$; Fig. 2e). Figure 2f represents males of different ages. No significant differences were found in entry into the periphery, time in the center and periphery in open field, and spatial memory performance was preserved in aging mice as observed in the T-maze test (see Supplementary Table 2 for results).

The interclass correlation coefficient (ICC) was calculated to ensure the reliability of the manually analyzed data, such as the frequency of rearing and grooming. According to the Cicchetti[42] scale, the results (See Supplementary Table 3) were deemed excellent (0.75 to 1.00).

Aging males show reduced sexual behavior. To assess this in our study model, a spontaneous social interaction test with synchronized 2 to 3 months old females, was conducted (Fig. 3a). The aging male group (19 and 24 months) showed less social interaction time ($p = 0.0104$; Fig. 3b) and a lower frequency of chasing the female ($p = 0.0029$; Fig. 3c). Both aging groups showed a trend toward a decrease in the frequency of mating attempts compared to the younger mice ($p = 0.0823$; Fig. 3d). Once again, the 24-month group exhibited reduced rearing frequency ($p = 0.019$) compared to the 4-months group. No difference was observed in grooming frequency ($p = 0.932$) between the age groups.

The Interclass Correlation Coefficient (ICC) was calculated for the observed variables in this test (see Supplementary Table 3).

Testicular and sperm function

Testosterone and testicular weight declined in aging male mice. For the immunoassay's analytical validation, an ELISA (Enzyme-Linked Immunosorbent Assay) was used. The male serum pool's slope coefficient (−45.41) was similar to the testosterone standard curve (−40.45, $F = 3.28$, $p = 0.11$), confirming parallelism. The assay showed a precision with 95 ± 10% hormone recovery and an 8.1% intra-assay variation. Serum testosterone levels showed a significant difference when comparing groups of different ages ($p = 0.018$; Fig. 4a). The 24- and 19-month groups exhibited lower serum testosterone levels than the 4-month group. The analytical validation of the immunoassay is provided in Supplementary Material S9.

Additionally, the control group exhibited higher left ($p = 0.011$) and right ($p = 0.025$) testicular weights when compared to the aging groups (Supplementary Table 4). Importantly, body weight did not differ between groups (Supplementary Table 4), reinforcing that the observed reductions in testicular weight are due to intrinsic testicular changes rather than systemic body weight effects.

Analysis of age-related changes in spermatogenesis revealed that the 19-month group showed a higher percentage of tail defects ($p = 0.0234$) and multiple defects ($p = 0.036$) compared to the 4 and 24-month groups (Fig. 4b and 4c). The 24-month group exhibited a higher percentage of cells with intermediate piece defects ($p = 0.0059$) than the 4 and 19-month groups (Fig. 4b and 4c). The aging groups had a higher percentage of individual defects ($p = 0.0001$) and total defects ($p = < 0.0001$; individual plus multiple defects) compared to the control group (Fig. 4b and 4c).

Moreover, 24-month-old males displayed a higher percentage of protamine deficiency (positive for CMA3; $p = 0.045$; Fig. 4d and 4e) when compared to 4 and 19-month groups. In the flow cytometry assessments, the 19-month males exhibited higher intermediate mitochondrial membrane potential ($p = 0.032$) and damaged plasma membrane with oxidative stress ($p = 0.003$) compared to the 4- and 24-month groups (see Supplementary Table 4).

No significant differences were found in the weight of males, sperm concentration, or other variables evaluated in sperm morphology assays, flow cytometry, Sperm Chromatin Susceptibility Assay modified, CASA and polyspermy rate among the age groups (see Supplementary Table 4).

To understand the etiology of the trend towards reduced fertilization rates ($p = 0.067$), the sperm capacitation process was analyzed using chlortetracycline assay (CTC) after in vitro induction. There was no difference between the experimental groups for non-capacitated sperm (CTC1; $p = 0.090$; Fig. 4f and 4g). The percentage of capacitated sperm (CTC2; $p = < 0.0001$; Fig. 4f and 4g) was decreased in the aging groups compared to the control group. The 19-month group showed an increase in sperm with acrosome reacted ($p = 0.016$; Fig. 4f and 4g) compared to the 4-month group.

Embryo development

Males aging impaired in vitro embryo development and blastocyst kinetics. We observed that the cleavage rate was lower for the 24-month group than the 4-month group ($p = 0.029$; Fig. 5a e 5b). The rates of blastocyst formation ($p = 0.007$) and embryo development ($p = 0.012$) were lower for the 24-month group compared to the 4 and 19-month groups (Fig. 5a and 5b). However, the 19-month group showed a higher rate of early blastocysts (EB; $p = 0.005$; Fig. 5c) than the 4 and 24-month groups. No difference was found in the blastocyst stage (BL; $p = 0.247$; Fig. 5c) among the experimental and the control groups. The aging groups had a lower expanded blastocyst rate (BX; $p = 0.040$; Fig. 5c) than the 4-month group. The rate of hatched blastocysts (HB; $p = 0.003$; Fig. 5c) differed among the age groups, with the aging groups showing a lower rate than the control.

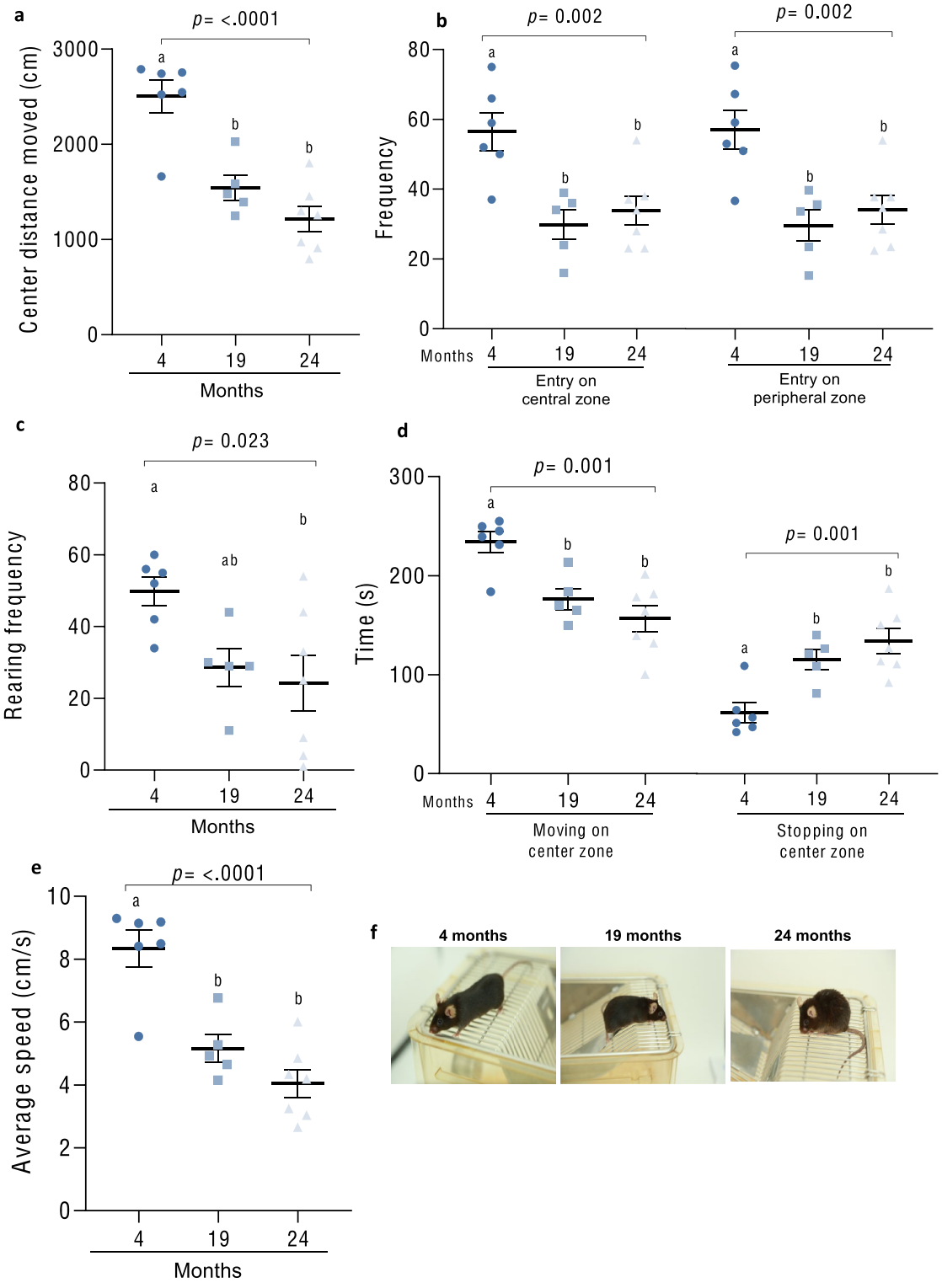


Fig. 2. Aging male mice exhibit reduced locomotor activity on the open field test. Parameters evaluated by the Ethovision XT imaging system among the 4-month (n = 6), 19-month (n = 5), and 24-month (n = 7) age groups. **a** center distance moved. **b** Frequencies of entry into the central and peripheral zone. **c** rearing frequency. **d** Times of moving and stopping in the central zone. e Average speed. f Representative image (EOS 5D Mark III DS126321, Canon®, Japan) of males from the age groups. Different superscript letters indicate significant differences ($p < 0.05$, ANOVA one-way test with post-hoc LSD). Error bars, mean ± SEM.

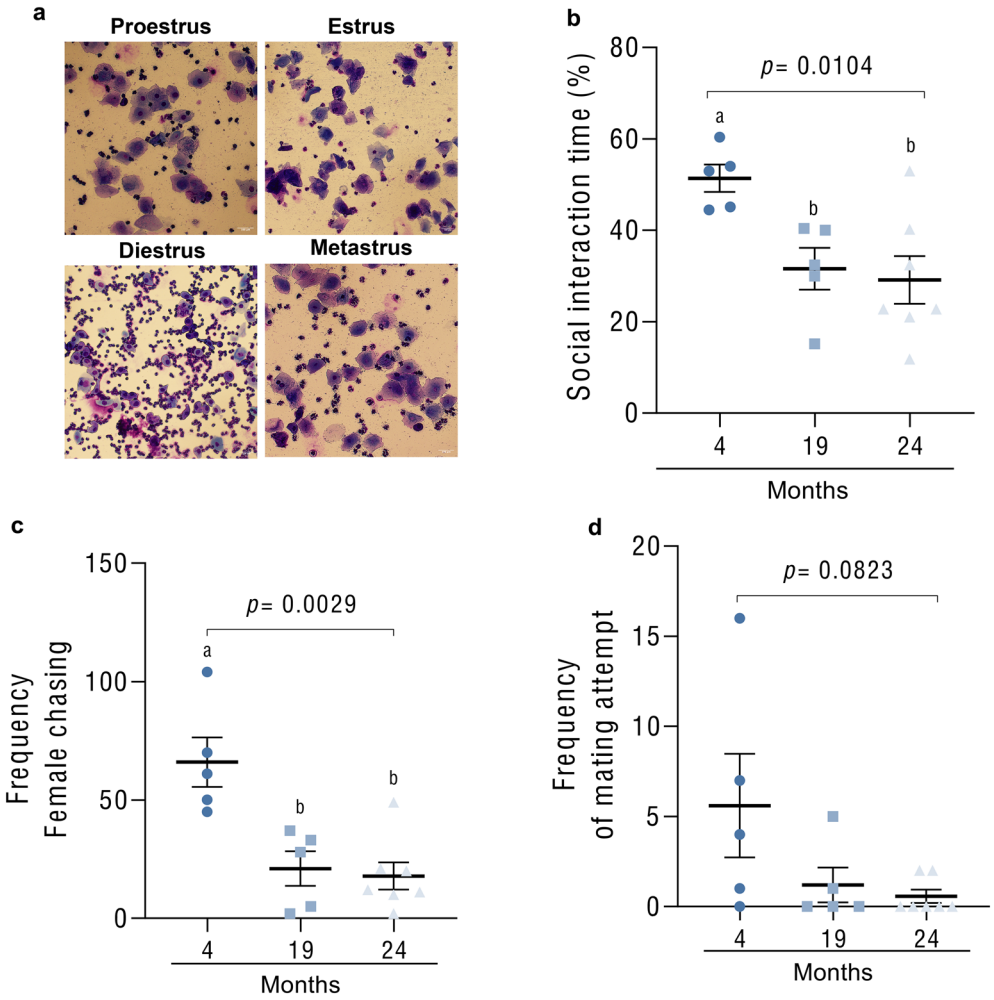


Fig. 3. Aging males show reduced sexual behavior **a** Morphological characterization of vaginal cells of each phase of the estrous cycle (estrus, proestrus, metestrus, and diestrus) in female mice (n = 17), under magnification of 400x (the scale bar represents 100 µm). Parameters assessed among the age groups of 4 months (n = 5), 19 months (n = 5), and 24 months (n = 7): **b** time of social interaction between males and females; **c** frequency of female chasing; **d** frequency of mating attempt. Different superscript letters indicate significant differences ($p < 0.05$, ANOVA one-way com post-hoc LSD). The dependent variable frequency of mating attempt showed a non-parametric distribution; the Kruskal–Wallis test was used, followed by pairwise comparisons using the Mann–Whitney test. Error bars, mean ± SEM.

Males aging compromise the first embryonic cell allocation. The 24-month male group showed a lower count of inner cell mass cells (ICM; $p = 0.035$; positive for SOX2; Fig. 6a and b) compared to the 4-month group. Both aging groups exhibited a lower count of trophectoderm cells (TE; $p = 0.016$; positive for CDX2; Fig. 6a and b) than the 4-month group. There was no significant difference in the ICM: TE ratio between the experimental groups ($p = 0.3552$; Fig. 6b). Both aging groups had a lower total cell count (positive for Hoechst 33,342; $p = 0.004$; Fig. 6a and c) compared to the control group.

The fluorescence intensity of these proteins was also measured as an indirect method to quantify protein expression. The aging groups showed lower CDX2 fluorescence intensity compared to the 4-month group ($p = < 0.0001$; Fig. 6d). The 24-month group exhibited lower SOX2 fluorescence intensity for the protein compared to the 4- and 19-month groups ($p = < 0.0001$; Fig. 6e). Additionally, 2 out of 12 embryos from the 24-month group did not show SOX2 staining.

Experiment 2

Fetal development

Considering the impact of paternal aging observed in experiment 1, we hypothesized that conceptus development could be compromised due to paternal aging at 16 days of gestation. Different males were used in this experiment since the animals in Experiment 1 were euthanized to collect semen. Additionally, due to logistical constraints, data for this experiment were not collected concurrently for the three age groups (4, 19, and 24 months), as was in Experiment 1.

To ensure similar experimental conditions between groups, the males were euthanized after mating, and their sperm was collected and analyzed using flow cytometry and CASA techniques, as described previously. The aim was to check for seminal abnormalities, as no differences were observed between age groups in Experiment 1. The evaluation of these new males confirmed the absence of differences (see Supplementary Table 5). It is important to note that two males from the 24-month-old group died due to comorbidities inherent to aging; therefore, their sperm was not evaluated.

The 24-month-old group produced smaller and lighter fetuses when compared to the control group. Additionally, the fetus-to-placenta weight ratio was lower in the 24-month-old compared to the control (Table 1).

In contrast, no significant differences were observed between the 19-month-old versus 4-month-old groups (Table 1). Furthermore, no significant changes were noted in placental assessments (Table 1) or litter size evaluations (Table 2).

For raw data, the number of viable fetuses, the number of resorption sites, altered fetuses, and total structures see Supplementary Table 6 (4 × 19 months) and Supplementary Table 7 (4 × 24 months).

Discussion

Building upon our previous findings[10], this study was designed to address unanswered questions regarding the impact of paternal aging on reproductive performance and offspring development. While our previous work established that male aging negatively affects fertility outcomes, it remained unclear when these changes begin, whether they emerge gradually from 19 months or become more pronounced at 24 months. Additionally, the behavioral and hormonal alterations underlying reproductive decline were not fully characterized. It was also unknown which specific sperm functional parameters contribute to impaired embryonic development. Moreover, given blastocyst formation was not absent in older males, we aimed to determine whether morphological and molecular differences exist among embryos from different paternal age groups.

To address the gaps from your previous studies, we evaluated behavioral, hormonal, sperm functional, and embryo development parameters in male mice at 4, 19, and 24 months contemporaneously. Our findings highlight that aging males exhibit significantly reduced psychomotor activity and reproductive interest, reduced serum testosterone levels, altered sperm morphology and protamination status, and a lower percentage of in vitro-capacitated spermatozoa. Furthermore, we observed lower embryo development rates, delayed embryonic kinetics, and impaired cell differentiation, leading to compromised fetal outcomes.

We observed that aged males exhibited reduced psychomotor activity in the open field test. This decrease may be attributed to age-related factors such as decreased muscle strength, reduced curiosity, and increased fear. Still, it may also be linked to lower cerebellar activity[43]. The increased speed in the control group may be due to the emergent need to seek food, primarily shelter. These findings align with previous studies with C57BL/6 mice 12 months[44,45], 18 to 20 months[46], 22 months[47], and 24 months[48] when compared to younger mice (2 to 6 months of age). This demonstrates the robustness of the open field test as an initial screening tool, even in the context of aging. Therefore, these results with the existing literature support the model.

Understanding male sexual interest is fundamental, given that population aging is an inherent phenomenon in all societies[49]. Studies have evaluated the synergy of aged male mice at 18[45] and 23 months[50] with other males, observing a decline in social interaction time. However, to our knowledge, the present study is the first to evaluate social interaction and reproductive interest in the experimental condition of aging. The social interaction test was adapted using hormonally synchronized females in estrus and proestrus, which proved effective in identifying behavioral differences in males'reproductive interests during aging.

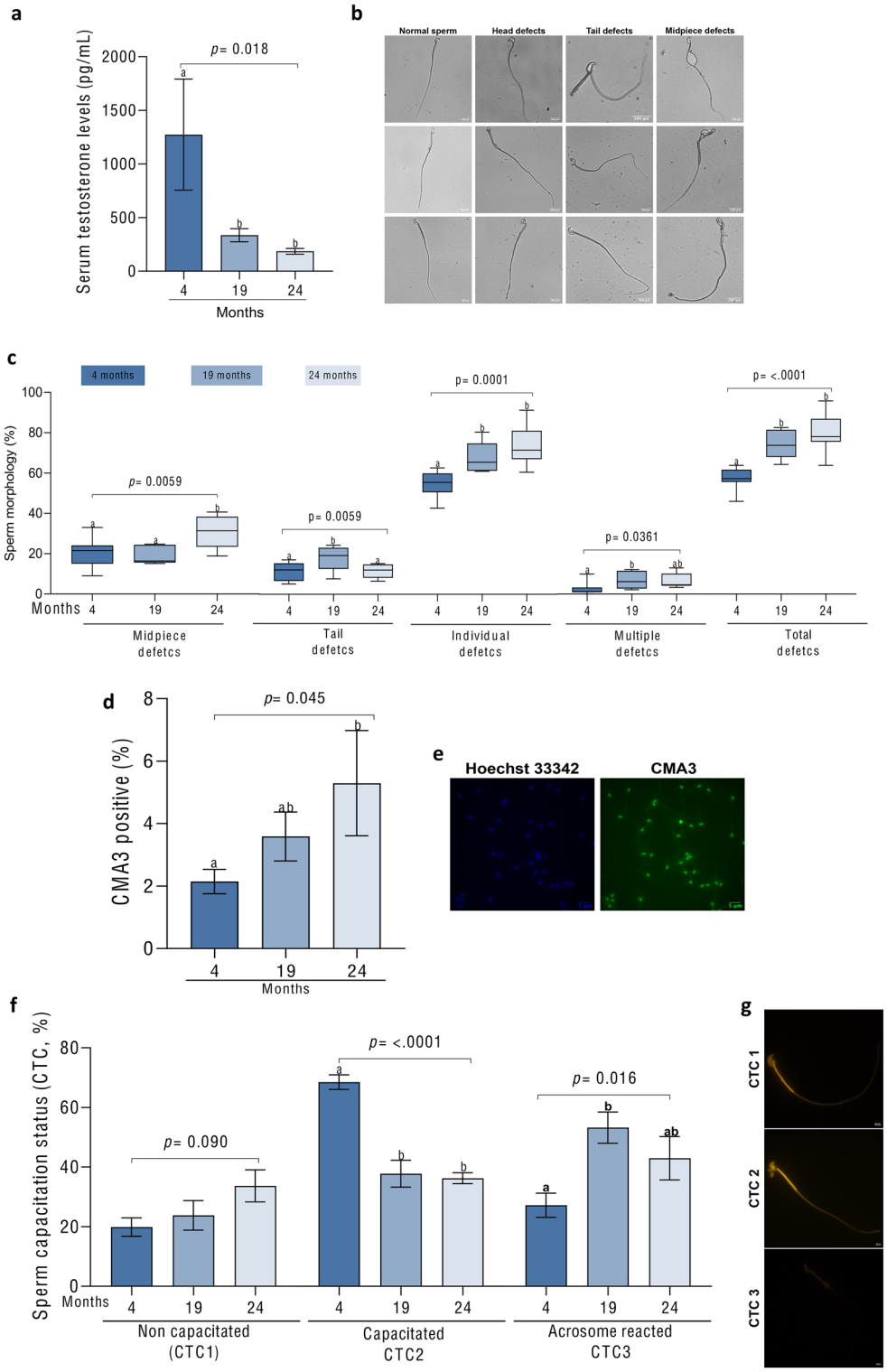
However, this decline was not absolute, suggesting that additional factors beyond behavior might contribute to reproductive impairments. One key aspect is hormonal regulation, as aged males showed lower serum testosterone levels, a critical hormone for male reproductive behavior. Testosterone decline is a well-documented aspect of aging in humans[12,51,52] and mice[13–16], which may contribute to decreasing libido and mating success observed in older males.

According to McBride et al.[53], testosterone deficiency in aging men affects Leydig cells and the hypothalamic-pituitary–gonadal (HPG) axis, disrupting hormone release. These factors may underlie the observed decrease in testicular weight in this study, a phenomenon also reported in mice[54] and humans[55,56] with advancing age.

This study reinforces that sperm quantity does not equate to quality, as aged males exhibited morphological defects despite unchanged sperm concentration. These abnormalities may originate from disruptions in spermatogenesis, including irregular meiosis and defective organelle transformations, or from impaired epididymal transit, which normally eliminates defective sperm[57,58]. Human studies suggested a 0.2–0.9% reduction in sperm morphology per year in men[59], a fourfold higher likelihood of abnormalities in men over 50[60] and an increase in the frequency of combined morphological defects observed in men over 40[21,61–63].

Unexpectedly, the 19-month-old group exhibited more functional alterations than the 24-month-old group, despite being an intermediate age. Reducing mitochondrial membrane potential can increase electron transport frequency to restore mitochondrial membrane potential. Thus, the intermediate mitochondrial membrane potential (sub-optimal) result observed in the 19-month age group may be related to this compensatory mechanism[64,65], but it can disrupt oxidative homeostasis, leading to sperm damage, including membrane damage. The absence of this compensatory mechanism in the 24-month group may be due to the more advanced age (the average lifespan of a C57BL/6 J is 29 months[37]), as their adaptive responses could be limited, supported by the increased defects observed in the sperm morphology. Endo et al.[40] also reported the absence of mitochondria in the midpiece of sperm from 24-month-old mice.

Additionally, sperm capacitation, a crucial process for fertilization, was disrupted in aged males. Diao et al.[66] reported that men aged 40 to over 60 showed reduced CFTR (cystic fibrosis transmembrane conductance regulator) protein levels in sperm, which is essential for bicarbonate influx and, consequently, for the



modulation of CatSper channels, ultimately influencing calcium signaling during capacitation, as detected by chlorotetracycline (CTC) staining[67,68]. The premature capacitation observed in the 19-month group may be linked to oxidative stress-induced[69] plasma membrane damage, leading to mitochondrial calcium leakage or dysregulation of calcium efflux channels, which could prematurely trigger capacitation.

The 24-month-old group exhibited alterations in protamination status, which we consider particularly severe, as protamines are essential for chromatin condensation and reactivation of gene transcription and the reprogramming of the embryonic genome[70,71]. The increased CMA3-positive spermatozoa in this group suggests defective histone-to-protamine replacement, aligning with previous studies showing age-related declines in PRM1 and PRM2 expression in mice and men[60]. This can result in the early decondensation of sperm chromatin[71], leading to failures in fertilization and subsequent embryonic development.

◂**Fig. 4**. Age-related changes in testosterone levels, testicular weight, spermatogenesis, and sperm capacitation **a** Serum testosterone levels among groups of 4- (n = 5), 19- (n = 4) and 24- (n = 5) month-old mice. **b** Representative image of the morphological classifications of normal sperm and the defects, at a magnification of 1000x, under immersion oil (the scale bar represents 200 µm). **c** Percentage of tail defects, midpiece defects, individual defects, multiple defects, and total defects among the age groups of 4 (n = 11), 19 (n = 5), and 24 (n = 8) months. **d** Percentage of spermatozoa positive in the CMA3 assay at 4 (n = 10), 19 (n = 5) and 24 (n = 8) months. **e** Representative image of spermatozoa stained with Hoechst 33,342 (nucleus) and cells positive for Chromomycin A3 (CMA3) at a magnification of 400x (the scale bar represents 5 µm). **f** Percentage of spermatozoa classified as CTC1, CTC2, and CTC3 among the age groups of 4 (n = 9), 19 (n = 5) and 24 (n = 9) months. **g** Representative image at a magnification of 1000 × under immersion oil of the CTC assay classifications (the scale bar represents 10 µm). Different superscript letters indicate significant differences ($p < 0.05$, ANOVA one-way com post-hoc LSD). The dependent variable, multiples defects, showed a non-parametric distribution; the Kruskal–Wallis test was used, followed by pairwise comparisons using the Mann–Whitney test. Error bars, mean ± SEM.

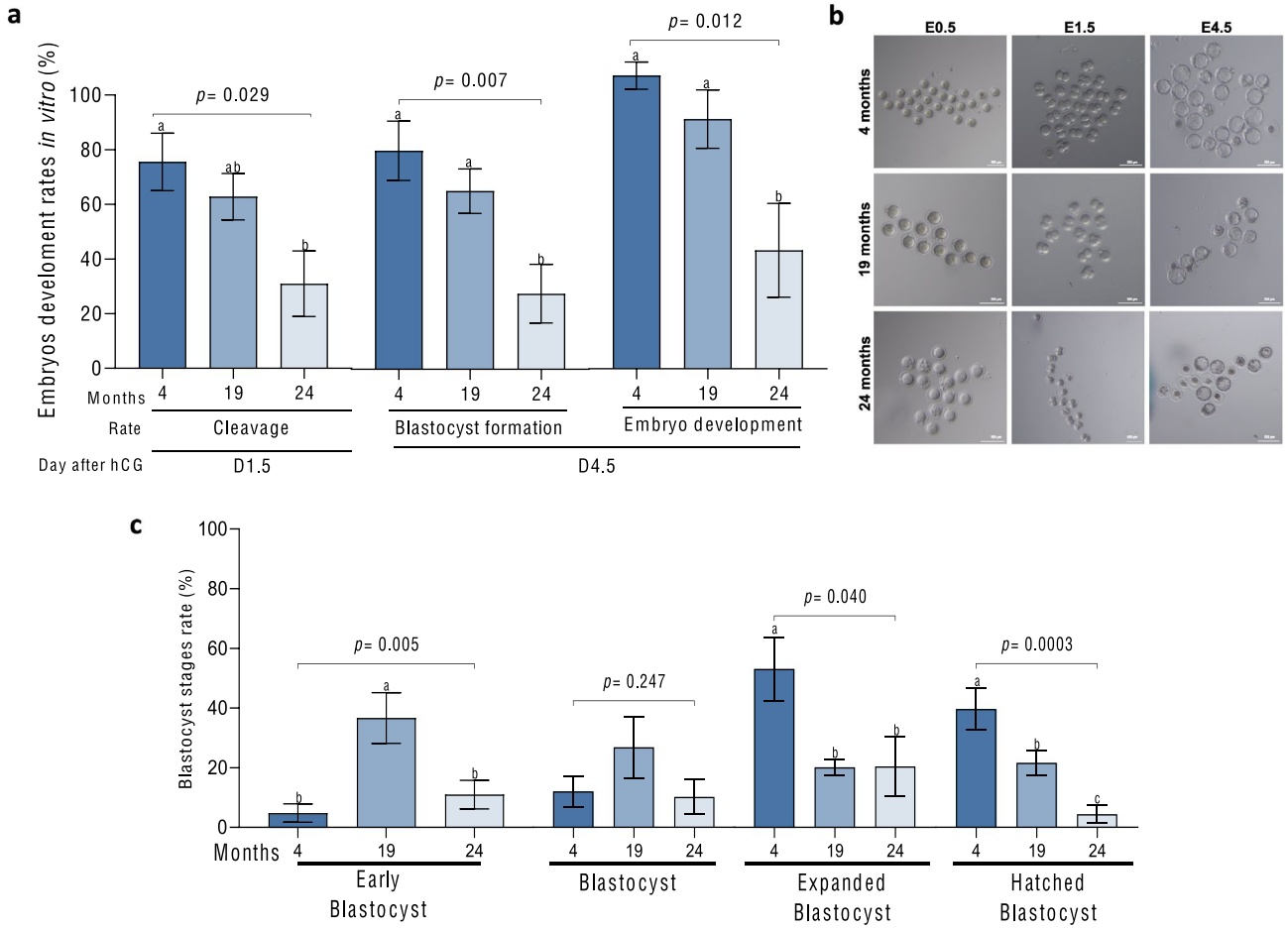


Fig. 5. Males aging impaired in vitro embryo development and blastocyst kinetics **a** In vitro embryo development among the age groups of 4 months (n = 5), 19 months (n = 5), and 24 months (n = 7): cleavage rate (number of cleaved embryos/total number of structures × 100), blastocyst formation rate (number of blastocysts/total number of structures × 100), embryo development rate (number of blastocysts/number of cleaved embryos × 100). **b** Representative image at a magnification of 60 × of presumed zygotes, cleaved embryos, and blastocysts among the age groups (the scale bar represents 500 µm). **c** Stages of blastocysts: early blastocyst (EB), blastocyst (BL), expanded blastocyst (BX), and hatched blastocyst (HB). Different superscript letters indicate significant differences ($p < 0.05$, Kruskal–Wallis test was used, followed by pairwise comparisons using the Mann–Whitney test). Error bars, mean ± SEM.

Theses alterations in capacitation and protamination status could explain both the trend toward a lower fertilization rate and the significant reduction in cleavage and blastocyst formation rate observed in our study. This aligns with our previous findings[10], where we reported a 35% and 89% reduction in the cleavage and blastocyst rate of embryos derived from C57BL/6 J male mice aged 18 to 24 months.

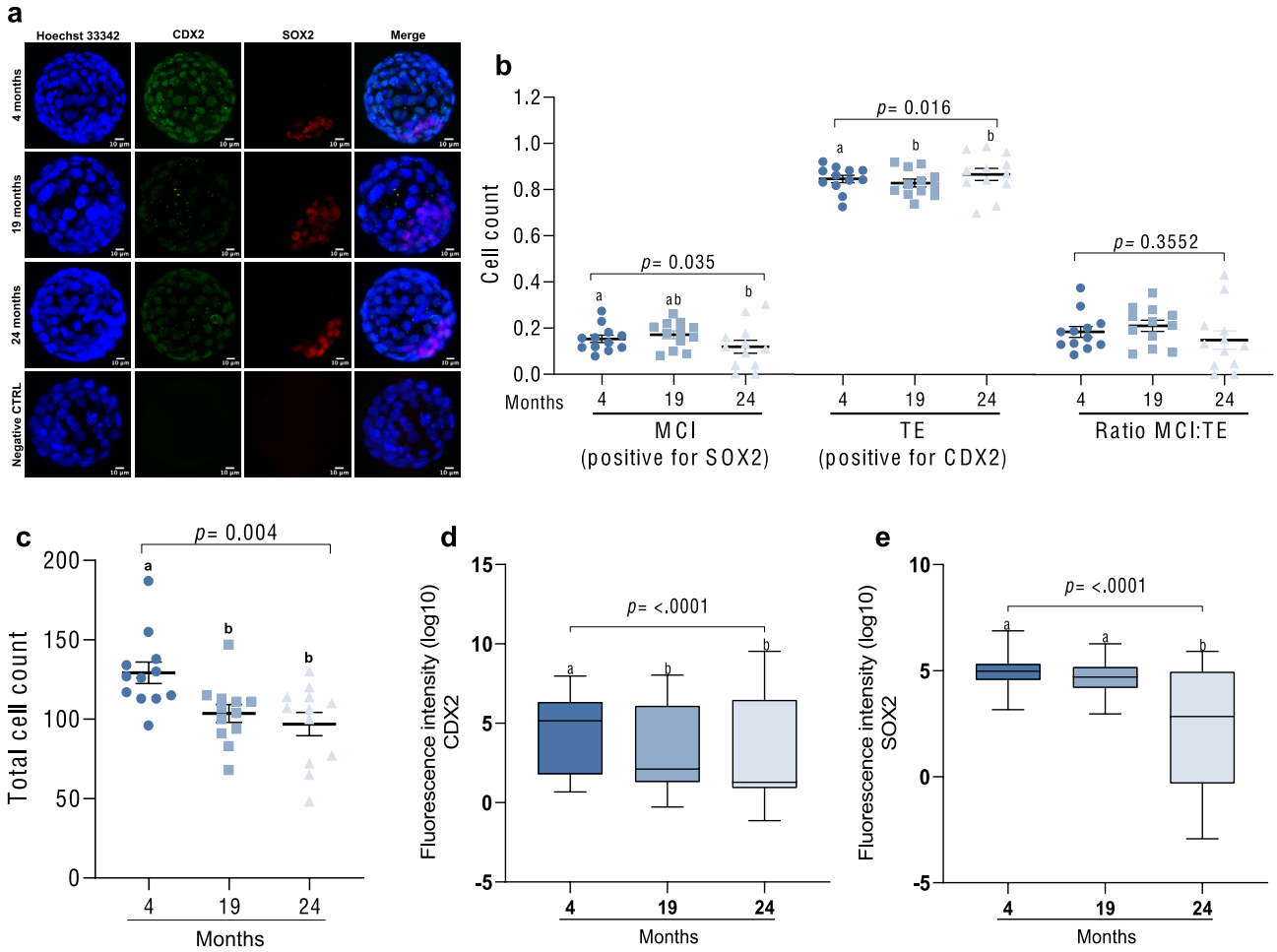


Fig. 6. Male aging compromises the first embryonic cellular differentiation **a** Z-stack images were converted into single maximum projection images (scale bars, 10 µm). **b** The ICM (positive for SOX2) and TE (positive for CDX2) cells count. **c** The total number of cells (positive for Hoechst 33,342) count. For cell counts, the experimental unit was embryos from males aged 4 (n = 12), 19 (n = 12), and 24 (n = 12). **d** Fluorescence intensity of CDX2 among the experimental groups. The experimental unit was nuclei from embryos of males aged 4 (n = 1330), 19 (n = 1036) and 24 (n = 1013) months. **e** Fluorescence intensity of SOX2 among the experimental groups. The experimental unit was nuclei from embryos of males aged 4 months (n = 234), 19 months (n = 208) and 24 months (n = 322). Different superscript letters indicate significant differences ($p < 0.05$, ANOVA one-way com post-hoc LSD). The dependent variables ICM count and SOX2 and CDX2 fluorescence intensity showed a non-parametric distribution; the Kruskal–Wallis test was used, followed by pairwise comparisons using the Mann–Whitney test. Error bars, mean ± SEM.

Variables	19 months n = 4	Control n = 6	*p*	24 months n = 12	Control n = 16	*p*
Fetuses weight (g)	0.23 ± 0.04	0.25 ± 0.02	0.63	**0.29 ± 0.02[a]**	**0.33 ± 0.01[b]**	**0.04**
Fetuses length (cm)	1.15 ± 0.07	1.18 ± 0.04	0.66	**1.24 ± 0.03[a]**	**1.30 ± 0.01[b]**	**0.03**
Placental weight (g)	0.08 ± 0.01	0.08 ± 0.00	0.68	0.13 ± 0.02	0.10 ± 0.00	0.30
Placental length (cm)	0.77 ± 0.02	0.76 ± 0.03	0.92	0.84 ± 0.01	0.84 ± 0.01	0.99
Placental area (cm2)	0.47 ± 0.03	0.46 ± 0.03	0.93	0.56 ± 0.02	0.56 ± 0.01	0.99
Fetal:placental weight ratio	2.85 ± 0.60	3.18 ± 0.24	0.57	**2.70 ± 0.26[a]**	**3.39 ± 0.11[b]**	**0.03**

Table 1. Fetuses and placental size at 16 days of gestation of male mice 19-months vs. 4-month groups and 24-months vs. 4-months. Legend: n = mean litter size. Different superscript letters represent $p < 0.05$, as a statistical T-test indicates.

Variables	19 months	Control	p	24 months	Control	p
	n = 5	n = 7		n = 13	n = 17	
Number of resorptions sites	3.60 ± 0.98	1.50 ± 0.29	0.11	2.92 ± 0.61	2.65 ± 0.37	0.69
Number of viable fetuses	7.67 ± 3.53	9.50 ± 1.03	0.53	4.00 ± 0.84	6.13 ± 0.78	0.08
Number of total structures	10.80 ± 3.25	12.50 ± 1.52	0.63	7.00 ± 1.04	8.59 ± 0.92	0.26

Table 2. Characteristics of the litter size at 16 days of gestation of male mice 19 months vs. 4 months and 24 months vs. 4 months. Legend: n = litter size (viable fetuses and/or only resorption sites) Different superscript letters represent $p < 0.05$, as a statistical T-test indicates.

Similarly, Gonzalez et al.[72] observed a 47% reduction in the cleavage rate of embryos from C57BL/6 mice over 14 months of age. Katz-Jaffe et al.[73] reported a decline in blastocyst formation and quality of expanded blastocysts in mice aged 12 to 15 months, accompanied by reduced PRM1 and PRM2 gene expression. Frattarelli et al.[74], in a study involving 1,023 men, found that from the age of 51, there was a decrease in blastocyst formation and an increase in gestational losses and live births, reinforcing the impact of paternal aging on reproductive outcomes.

Although the senile group was able to fertilize, cleave, and reach the blastocyst stage, age influenced the kinetics and efficiency of this development. This was evidenced by a higher rate of early blastocysts (EB) at D4.5, while physiologically, the embryos should already be expanded or hatching at this stage[75,76]. In humans, slower-growing embryos are associated with higher aneuploidy rates[77]. This delay in development may be related to the transfer of messenger RNAs (mRNA) and non-coding RNAs (ncRNA) from the sperm to the oocyte during fertilization. Studies have shown that, in mice, the absence of sperm ncRNAs delays the first cleavage[78] and cell proliferation[79,80].

In mice, the blastocyst progresses from the early blastocyst at D3.5 to the expanded blastocyst at D4.5, containing about 140 cells capable of implantation[81]. Based on these results, the impairment of implantation may occur due to the reduced number of cells observed in this study. Endo et al.[40] also reported a decrease in the total number of cells in TE and ICM in mice aged from 24 to 26 months.

Although the mechanisms by which advanced paternal age affects first-cell differentiation are not fully understood, the consequences are clear. In the present study, two blastocysts from the 24-month group did not show SOX2 marking and appeared to have normal morphology. Supporting this, Avilion et al.[82] suggest that the absence of SOX2 does not prevent blastocyst formation but reduces the expression of essential TE transcripts, such as CDX2[83]. Additionally, Wicklow et al.[84] observed that blastocysts lacking SOX2 have reduced SOX17, a marker of primitive endoderm, which will eventually give rise to extraembryonic tissues such as the yolk sac and the visceral endoderm.

In the second experiment, our objective was to verify whether paternal aging continued to influence the development after embryo implantation. The results indicated that fetuses from the 24-month group were smaller and lighter than those from the 4-month group, and they also had a lower ratio of fetal weight to placental weight.

These findings are in line with previous studies conducted on aged male mice, which demonstrated a decrease in litter size[40,73] and placental and fetal alterations[10,72,73,85] compared to younger males.

The reduced length and weight of the fetuses in the 24-month group may be linked to the reduction in the total cell number of blastocysts observed in the first experiment. Furthermore, the ICM, which will eventually give rise to the embryo itself, exhibited fewer cells and lower expression of SOX2, which is essential for pluripotency. This finding is consistent with Licciardi et al.[86] in humans, who demonstrated that blastocysts with a higher number of cells in the inner cell mass (ICM), classified according to the Gardner and Lane criteria, are predictive of greater fetal growth throughout gestation and at birth. A recent study[87] on human in vitro-produced (IVP) embryos observed a decline in blastocyst quality, including reductions in ICM, trophectoderm (TE), and embryonic expansion stage, ultimately leading to lower birth weight.

The results of our study increase the evidence that paternal aging negatively affects embryonic and fetal development by tracing a sequence of events that includes alterations in sexual behavior, sperm quality, and early embryo development, culminating in consequences for fetal growth.

Methods

Reagents and solutions

Unless otherwise indicated, all chemical reagents and solutions used in this study were purchased from Sigma-Aldrich (St. Louis, Missouri, USA).

Experimental design

This study was conducted following the ARRIVE guidelines[88] and all methods were performed in accordance with relevant guidelines and regulations. The study was approved by the Ethics Committee on the Use of Animals of the School of Veterinary Medicine and Animal Science of the University of Sao Paulo (under grants 3,336,011,221 and 7,125,160,518).

We used C57BL/6 J virgin male and female mice from the conventional house system of the Animal Facility from the Department of Animal Reproduction, School of Veterinary Medicine and Animal Science, University of São Paulo. The animals (experiment 1: total males = 25; total females = 52; experiment 2: total males = 43; total females = 69) were housed in individually ventilated cages (IVCs) measuring 30 cm (length) × 20 cm (width) × 13 cm (height), with a floor area of 451 cm^2 (ALESCO®, São Paulo, Brazil). The cages were lined with 2.5 cm of wood flake bedding (Good Life™, Granja RG, SP, Brazil) and maintained at a controlled temperature

of 22–24 °C, under a 12-h light/12-h dark cycle. Mice were provided irradiated commercial pellet food (Nuvilab CR-1™, Quimtia, Paraná, Brazil) and filtered water ad libitum, along with environmental enrichment using cardboard rolls and shredded paper.

The experimental design consisted of two contemporary blinded experiments involving 4 months (control group) and 19- and 24-month-old males (experimental groups) and young females (2 to 3 months) for mating. In Experiment 1, males from all three age groups (4, 19, and 24 months) were evaluated for behavioral, sperm, and in vitro embryo development analyses using the same animals for all assessments. In Experiment 2, in vivo fetal development was assessed using different males, with comparisons made between the 4-month and 19-month groups and the 4-month and 24-month groups, ensuring that all groups were contemporaneous.

The males were only individualized at the beginning of the experiments, and during the aging process, they remained in groups of 3 to 4 individuals to reduce stress and behavioral changes. The mice were monitored during the study according to the scoring table provided in Supplementary Table 1. Observations focused on their general health and any injuries caused by fighting. Only mice that showed no signs of aggression toward their cage mates and maintained good health were included in the study, while those exhibiting sporadic aggressive behavior were excluded from the experiment, aiming to minimize animal suffering and enhance the accuracy of the experiments[89].

Behavioral assessments

Male behavioral patterns were evaluated using three tests: open field test, T-maze alternation test and spontaneous social interaction test with synchronized females.

The open field test was used to assess exploratory and anxiety behavior and locomotor activity. Mice were placed in a circular arena, and their spontaneous behavior was recorded for 5 min. The protocol was described by Garcia-Gomes et al.[90]. The videos were analyzed using imaging software (Ethovision XT, version 15.0.1416, Noldus Information Technology, Netherlands).

The T-maze alternation test (protocol[90]) evaluated the spatial memory. Mice were placed in a T-shaped maze and allowed to explore, with their choices between arms recorded over five opportunities. A higher alternation rate was indicative of normal exploratory behavior, while a lower rate suggested cognitive rigidity.

The spontaneous social interaction test assessed male–female interaction, with females synchronized to the proestrus/estrus stage via hormonal treatment. Males were placed with a female in the open field arena for 10 min. Two blinded evaluators manually recorded the following parameters: interaction time ([interaction time (s)/total test time (s) × 100 (%)], frequency of female chasing and mating attempts, frequency rearing and grooming during the total contact time between the male and female.

To ensure the reliability and consistency of the manually analyzed results, the agreement between the evaluations was measured using the Interclass Correlation Coefficient (ICC), allowing us to verify whether both evaluators analyzed the data similarly. We followed Cicchetti's (1994) guidelines for interpreting ICC values, classified as follows: < 0.40 = poor, 0.40–0.59 = fair, 0.60–0.74 = good, and 0.75–1.00 = excellent.

For more details on the protocols, see Supplementary Material S1.

Euthanasia procedure

For the experiments involving embryo collection on embryonic day 0.5 (E0.5), females were euthanized solely by cervical dislocation to avoid any influence of anesthesia on embryo development[92]. For experiments involving fetal collection on day 16.5 (E16.5) of gestation, females were euthanized with an anesthetic overdose of Ketamine (150 mg/kg, Dopalen, Ceva®, Brazil), Xylazine (20 mg/kg, Anasedan, Ceva®, Brazil), and Acepromazine (3 mg/kg, Apromazin, Syntec®, Brazil), followed by cervical dislocation, to minimize fetal suffering. All male mice were euthanized only by cervical dislocation to avoid possible alterations in the semen.

Embryo development

For in vivo fertilization rate and in vitro embryo development, superovulated (protocol see Supplementary Material S2) young females that mated with males from the age groups were euthanized on E0.5 approximately 24 h after the administration of hCG. The collection of presumed zygotes followed the protocol of Stábile et al.[10]. Fixed presumed zygotes (2–6 per male) were stained with 10 µg/mL of the Hoechst 33,342 probe to determine the fertilization rate (number of fertilized/number of presumed zygotes × 100) and polyspermy (number of polyspermic/number of presumed zygotes × 100). For more details see Supplementary Material S3.

The zygotes were in vitro cultured (IVC) in KSOM medium (EmbryoMax, MR-106-D, Merck Millipore®, USA), covered with mineral oil (FUJIFILM, Irvine Scientific®, USA) and kept at 37 °C, 5% CO_2, 5% O_2, and 90% N_2 under high humidity, for 4.0 days, until reaching E4.5.

On day E1.5 of IVC, the cleavage rate (number of cleaved embryos/total structures × 100) was evaluated. On E4.5, the total blastocyst formation rate (number of blastocysts/total structures × 100) was analyzed. This included the assessment of specific blastocyst stages: early blastocyst (EB, blastocoel < 50% relative to the embryo), blastocyst (BL; blastocoel > 50% relative to the embryo), expanded blastocyst (BX, blastocoel > 50% relative to the embryo and defined inner cell mass), and hatched blastocyst (HB; blastocoel > 50% relative to the embryo, defined inner cell mass, and zona pellucida rupture). The embryo development rate (amount of blastocysts/number of cleaved embryos × 100) was evaluated. All analyses used a stereomicroscope (Olympus SZ61, Olympus®, Tokyo, Japan) with 60 × magnification. In this experiment, the experimental unit was the male, and the average data from males given two opportunities was calculated.

For immunostaining (protocol see Supplementary Material S4) randomly, 12 blastocysts (experimental units) from each age group were selected. The immunofluorescence was performed as previously described[91] for double staining the Caudal Type Homeobox 2 (CDX2) protein to and Sex-Determining Region Y-Box Protein 2 (SOX2) protein, markers of the TE and the ICM, respectively. Embryos were analyzed via confocal microscopy

(TCS SP8—STED 3X, Leica Microsystems®, Wetzlar, Germany) at CAIMi, at the Institute of Biosciences, University of Sao Paulo. Using the LAS X Life Science software, images were acquired every 10 µm to allow for three-dimensional reconstruction.

The fluorescence intensity of CDX2 and SOX2, as well as the differential analysis of blastocyst cells, were performed using ImageJ-Fiji software (National Institutes of Health, Bethesda, USA, https://imagej.nih.gov/ij/93). This analysis identified the following: (I) TE (positive for CDX2), (II) ICM (positive for SOX2), (III) total cells (positive for Hoechst 33,342), and the ICM:TE ratio. For more details see Supplementary Material S5.

Fetal development on the 16th day of gestation

All young females were euthanized on the 16th day of gestation to assess fetal development. The female reproductive tract was accessed, and fetuses were collected as described previously[10].

We evaluated the total number of structures (including viable fetuses and resorption sites), viable fetuses compatible with the gestational age at E16.5, and resorption sites. The conceptus (fetuses and their extraembryonic tissues) was removed and weighed on a digital analytical balance (model AG245, Marshall Scientific®, Hampton, USA), and the fetal: placental weight ratio was calculated. Photos of the fetuses and placentas were taken using a digital color camera (Olympus LC30, Olympus®, Munster, Germany) attached to a stereomicroscope (Olympus SZ61, Olympus®, Tokyo, Japan). Measurements of fetal length (crown to rump) and placental length and area (the circle drawing tool was used to delineate the tissue area, and the software automatically calculated the area in square micrometers [µm^2]) were performed using CellSens® Software (Olympus Live Science, Olympus®, Tokyo, Japan).

Sperm collection, count, and morphology

The males were euthanized, and semen was collected from the epididymal cauda and the vas deferens following the protocol from Stábile et al.[10]. To each male semen, 200 µL of CZB-Hepes medium was added. For sperm morphology assessment, 5 µL of diluted semen was fixed in 10% formalin saline buffered with PBS, and a total of 100 spermatozoa per sample (male) were subsequently evaluated under a phase-contrast microscope (Olympus CH30, Olympus®, Tokyo, Japan) at 1000 × magnification, using mineral oil immersion. Sperm abnormalities were classified into individual defects, acrosome defects, head defects, midpiece defects, and tail defects (adapted from[92–95] and multiple defects (sperm with more than one abnormality simultaneously). Subsequently, sperm concentration (1:20) was measured using a hemocytometer and then diluted to a final concentration of 25×10^6 sperm/mL for analyses performed by flow cytometry.

CASA: Sperm coordination, motility, and velocity analysis

Sperm kinematics were assessed using the Computer Assisted Sperm Analysis (CASA; Hamilton-Thorne®, Ivos 12.3, USA) using the equipment murine procedure. An aliquot (3 µL) of each sample was inserted into a Leja® counting chamber previously heated to 37 °C and at least 1,000 cells in a minimum of six fields per sample were selected for the analysis (setup for evaluating mouse sperm kinematics see Supplementary Table 8). The variables assessed were: (1) percentages of total motility spermatozoa (TM. %); (2) spermatozoa with progressive motility (PROG. %); (3) average pathway velocity (VAP. µm/s); (4) straight-line velocity (VSL. µm/s); (5) curvilinear velocity (VCL. µm/s); (6) amplitude of lateral head displacement (ALH. µm); (7) beat cross frequency (BCF. Hz); (8) straightness (STR. %) of sperm movement; and (9) linearity (LIN. %). Sperm were also classified based on velocity: rapid (RAP, VAP > 50 µm/s. %); medium (MED, 30 µm/s < VAP < 50 µm/s. %); slow (SLOW, VAP < 30 µm/s or VSL < 15 µm/s. %); and static (STATIC. %), non-moving spermatozoa[96].

Flow cytometer: Plasma and acrosome membrane integrity, mitochondrial membrane potential, oxidative status analysis and sperm chromatin susceptibility assay modified (SCSAm)

The plasma membrane integrity (propidium iodide; PI) and acrosomal integrity (fluorescein isothiocyanate conjugated with Pisum sativum agglutinin; FITC-PSA), mitochondrial membrane potential (5,5',6,6'-tetrachloro-1,1,3,3'-tetraethylbenzimidazolylcarbocyanine iodide; JC-1), oxidative stress (CellRox green® probe) and sperm's susceptibility to DNA fragmentation (SCSAm; protocol see Supplementary Material S6) were evaluated by flow cytometry (Guava Easy Cyte™ Mini System, Guava Technologies®, Hayward, CA, USA). Data were analyzed using Flowjo™ v8.7 software (Flow Cytometry Analysis Software® —Tree Star Inc., Ashland, Oregon, USA), following the protocol described by Stábile et al.[10].

Chromomycin A3 (CMA3): Sperm chromatin condensation

The protocol described by Castro et al.[97] was adapted (for more details see Supplementary Material S7). A final concentration of 25 million spermatozoa/mL was used. Slides were observed using an inverted epifluorescence microscope (Olympus IX80, Olympus®, Tokyo, Japan) under ultraviolet light excitation at 400 × magnification. The total sperm count (at least 150 cells) was obtained using the blue filter (U-MWU2; 345 nm excitation and 455 nm emission), and CMA3-positive sperm were counted using the green filter (U-MWB2; 495 nm excitation and 519 nm emission).

In vitro induction and evaluation of sperm capacitation status

For in vitro sperm capacitation induction, the diluted semen was incubated in the medium Human Tubal Fluid with calcium for 1 h at 37 °C with 5% CO_2 in air. After the sperm capacitation period, a chlortetracycline (CTC) probe was used (protocol adapted[67,98]). Approximately 100 spermatozoa were assessed at 1000 × magnification under mineral oil using an inverted epifluorescence microscope (Olympus IX80, Olympus®, Tokyo, Japan). The cells were classified: CTC 1—non-capacitated (yellow fluorescence throughout the head); CTC 2—capacitated

(yellow fluorescence only in the acrosomal region); and CTC 3—acrosome reacted (intense fluorescent band in the equatorial region or without fluorescence emission). for more details see Supplementary Material S8.

Measurement of serum testosterone levels

Serum samples from males aged 4 months (n = 5), 19 months (n = 4), and 24 months (n = 5) who participated in experiment 1 were used. The procedures were carried out at the Hormonal Assays Laboratory (LDH, FMVZ, USP), following a protocol adapted[99]. To minimize matrix effects, samples were treated according to the manufacturer's recommendations for the enzyme immunoassay (EIA; DetectX K032, Arbor Assays™, Eisenhower Place, Ann Arbor, MI, USA). For more details on the protocol and validation see Supplementary Material S9.

Statistical analysis

Statistical analysis was performed using the Statistical Analysis System 9.4 software (SAS Institute, Cary, NC, USA). The samples were tested for normality of residuals and homogeneity of variances using the SAS Guided Data Analysis tool. To compare three groups (Experiment 1—4, 19, and 24 months), one-way ANOVA with the Least Significant Difference (LSD) post hoc test was used. Post hoc comparisons were made between each group individually to evaluate the differences. When comparing two groups (Experiment 2—4 vs. 19 and 4 vs. 24 months), the two-tailed Student T-Test was employed. In cases of non-parametric data, the Kruskal–Wallis test was employed, followed by pairwise comparisons using the Mann–Whitney test. The probability (p) values are presented along with the results for each variable, considering a significance level of 0.05 to reject the null hypothesis. The data are presented as mean ± SEM (standard error of the mean). The graphs were generated using GraphPad Prism (version 5.0, Windows, USA).

ICC statistical analysis was performed using IBM SPSS Statistics software, Version 30.0.0 (IBM Corp., Armonk, NY, USA).

Data availability

The datasets analyzed during the current study are available from the corresponding author upon reasonable request.

Received: 8 January 2025; Accepted: 23 June 2025
Published online: 01 July 2025

References

1. Bray, I., Gunnell, D. & Smith, G. D. Advanced paternal age: How old is too old?. *J. Epidemiol. Commun. Health* **1978**(60), 851–853 (2006).
2. Ha, A. S. et al. Sociodemographic trends and perinatal outcomes in fathers 50 years and older. *JAMA Netw. Open* **7**, e2425269 (2024).
3. Mazuy, M., Barbieri, M., Breton, D. & D'Albis, H. The demographic situation in France: Recent developments and trends over the last 70 years. *Population (Wash DC)* **70**, 393–460 (2015).
4. DESTATIS. Fathers aged 34.6 years on average when children are born. https://www.destatis.de/EN/Press/2020/10/PE20_411_12.html (2020).
5. Neeser, N. B. et al. Building a family at advanced parental age: A systematic review on the risks and opportunities for parents and their offspring. *Hum. Reprod. Open* **2023**, hoad42 (2023).
6. Mac Dougall, K., Beyene, Y. & Nachtigall, R. D. 'Inconvenient biology': Advantages and disadvantages of first-time parenting after age 40 using in vitro fertilization. *Hum. Reprod.* **27**, 1058–1065 (2012).
7. Martins da Silva, S. & Anderson, R. A. Reproductive axis ageing and fertility in men. *Rev. Endocr. Metab. Disord.* **23**, 1109–1121 (2022).
8. Ferrini, M. G., Gonzalez-Cadavid, N. F. & Rajfer, J. Aging related erectile dysfunction—potential mechanism to halt or delay its onset. *Transl. Androl. Urol.* **6**, 20–27 (2017).
9. Feldman, H. A., Goldstein, I., Hatzichristou, D. G., Krane, R. J. & McKinlay, J. B. Impotence and its medical and psychosocial correlates: Results of the massachusetts male aging study. *J. Urol.* **151**, 54–61 (1994).
10. Stábile, L. A. et al. Paternal age impairs in vitro embryo and in vivo fetal development in murine. *Sci. Rep.* **12**, 13031 (2022).
11. García-Palomares, S. et al. Delayed fatherhood in mice decreases reproductive fitness and longevity of offspring1. *Biol. Reprod.* **80**, 343–349 (2009).
12. Harman, S. M., Metter, E. J., Tobin, J. D., Pearson, J. & Blackman, M. R. Longitudinal effects of aging on serum total and free testosterone levels in healthy men. *J. Clin. Endocrinol. Metab.* **86**, 724–731 (2001).
13. Lacombe, A. et al. Delayed testicular aging in pituitary adenylate cyclase-activating peptide (PACAP) null mice. *Proc. Natl. Acad. Sci.* **103**, 3793–3798 (2006).
14. Machida, T., Yonezawa, Y. & Noumura, T. Age-associated changes in plasma testosterone levels in male mice and their relation to social dominance or subordinance. *Horm. Behav.* **15**, 238–245 (1981).
15. Zhao, X. et al. Effects of moderate exercise over different phases on age-related physiological dysfunction in testes of SAMP8 mice. *Exp. Gerontol.* **48**, 869–880 (2013).
16. Gosden, R. G., Richardson, D. W., Brown, N. & Davidson, D. W. Structure and gametogenic potential of seminiferous tubules in ageing mice. *Reproduction* **64**, 127–133 (1982).
17. Neaves, W. B., Johnson, L., Porter, J. C., Parker, C. R. & Petty, C. S. Leydig cell numbers, daily sperm production, and serum gonadotropin levels in aging men*. *J. Clin. Endocrinol. Metab.* **59**, 756–763 (1984).
18. Dong, S. et al. Testicular aging, male fertility and beyond. *Front. Endocrinol. (Lausanne)* **13**, 1012119 (2022).
19. Fabricant, J. D. & Parkening, T. A. Sperm morphology and cytogenetic studies in ageing C57BL/6 mice. *Reproduction* **66**, 485–489 (1982).
20. Aitken, R. J. The amoroso lecture the human spermatozoon - a cell in crisis?. *Reproduction* **115**, 1–7 (1999).
21. Crow, J. F. The origins, patterns and implications of human spontaneous mutation. *Nat. Rev. Genet.* **1**, 40–47 (2000).
22. Pohl, E., Gromoll, J., Wistuba, J. & Laurentino, S. Healthy ageing and spermatogenesis. *Reproduction* **161**, R89–R101 (2021).
23. Jenkins, T. G., Aston, K. I. & Carrell, D. T. Sperm epigenetics and aging. *Transl. Androl. Urol.* **7**, S328–S335 (2018).
24. Eskenazi, B. et al. The association of age and semen quality in healthy men. *Hum. Reprod.* **18**, 447–454 (2003).
25. Kumar, N., Singh, A. K. & Choudhari, A. R. Impact of age on semen parameters in male partners of infertile couples in a rural tertiary care center of central India: A cross-sectional study. *Int. J. Reprod. Biomed.* **15**, 497–502 (2017).

26. Pino, V., Sanz, A., Valdés, N., Crosby, J. & Mackenna, A. The effects of aging on semen parameters and sperm DNA fragmentation. *JBRA Assist. Reprod.* **24**, 82 (2020).
27. Sloter, E. et al. Quantitative effects of male age on sperm motion. *Hum. Reprod.* **21**, 2868–2875 (2006).
28. Alio, A. P. et al. The effect of paternal age on fetal birth Outcomes. *Am. J. Mens Health* **6**, 427–435 (2012).
29. du Fossé, N. A., van der Hoorn, M.-L.P., van Lith, J. M. M., le Cessie, S. & Lashley, E. E. L. O. Advanced paternal age is associated with an increased risk of spontaneous miscarriage: A systematic review and meta-analysis. *Hum. Reprod. Update* **26**, 650–669 (2020).
30. Sharma, R. et al. Effects of increased paternal age on sperm quality, reproductive outcome and associated epigenetic risks to offspring. *Reprod. Biol. Endocrinol.* **13**, 35 (2015).
31. García-Ferreyra, J. et al. High aneuploidy rates observed in embryos derived from donated oocytes are related to male aging and high percentages of sperm DNA fragmentation. *Clin. Med. Insights Reprod. Health* **9**, CMRH-S32769 (2015).
32. Strom-Roum, E. M., Haavaldsen, C., Tanbo, T. G. & Eskild, A. Paternal age, placental weight and placental to birthweight ratio: A population-based study of 590 835 pregnancies. *Hum. Reprod.* **28**, 3126–3133 (2013).
33. Hubert, A., Szöke, A., Leboyer, M. & Schürhoff, F. Âge paternel élevé et risque de schizophrénie. *Encephale* **37**, 199–206 (2011).
34. D'Onofrio, B. M. et al. Paternal age at childbearing and offspring psychiatric and academic morbidity. *JAMA Psychiat.* **71**, 432–438 (2014).
35. Lyall, K. et al. The association between parental age and autism-related outcomes in children at high familial risk for autism. *Autism. Res.* **13**, 998–1010 (2020).
36. Fagundes, D. J. & Taha, M. O. Modelo animal de doença: Critérios de escolha e espécies de animais de uso corrente. *Acta. Cir. Bras.* **19**, 59–65 (2004).
37. Carrageta, D. F. et al. Animal models of male reproductive ageing to study testosterone production and spermatogenesis. *Rev. Endocr. Metab. Disord.* **23**, 1341–1360 (2022).
38. García-Palomares, S. et al. Long-term effects of delayed fatherhood in mice on postnatal development and behavioral traits of offspring1. *Biol. Reprod.* **80**, 337–342 (2009).
39. Mao, Y. et al. Advanced paternal age increased metabolic risks in mice offspring. *Biochimica et Biophysica Acta (BBA) – Mol. Basis Dis.* **1868**, 166355 (2022).
40. Endo, T. et al. Multiple ageing effects on testicular/epididymal germ cells lead to decreased male fertility in mice. *Commun. Biol.* **7**, 16 (2024).
41. Dutta, S. & Sengupta, P. Men and mice: Relating their ages. *Life Sci.* **152**, 244–248 (2016).
42. Cicchetti, D. V. Guidelines, criteria, and rules of thumb for evaluating normed and standardized assessment instruments in psychology. *Psychol. Assess* **6**, 284–290 (1994).
43. Bernard, J. A. & Seidler, R. D. Moving forward: Age effects on the cerebellum underlie cognitive and motor declines. *Neurosci. Biobehav. Rev.* **42**, 193–207 (2014).
44. Davis, M. J., Haley, T., Duvoisin, R. M. & Raber, J. Measures of anxiety, sensorimotor function, and memory in male and female mGluR4−/− mice. *Behav. Brain Res.* **229**, 21–28 (2012).
45. Shoji, H., Takao, K., Hattori, S. & Miyakawa, T. Age-related changes in behavior in C57BL/6J mice from young adulthood to middle age. *Mol. Brain* **9**, 11 (2016).
46. Benice, T. S., Rizk, A., Kohama, S., Pfankuch, T. & Raber, J. Sex-differences in age-related cognitive decline in C57BL/6J mice associated with increased brain microtubule-associated protein 2 and synaptophysin immunoreactivity. *Neuroscience* **137**, 413–423 (2006).
47. Yanai, S. & Endo, S. Functional aging in male C57BL/6J mice across the life-span: A systematic behavioral analysis of motor, emotional, and memory function to define an aging phenotype. *Front. Aging Neurosci.* **13**, 697621 (2021).
48. Lalonde, R. & Strazielle, C. Exploratory activity and motor coordination in old versus middle-aged C57BL/6J mice. *Arch. Gerontol. Geriatr.* **49**, 39–42 (2009).
49. Bloemers, J. et al. Toward personalized sexual medicine (Part 1): Integrating the "Dual Control Model" into differential drug treatments for hypoactive sexual desire disorder and female sexual arousal disorder. *J. Sex Med.* **10**, 791–809 (2013).
50. Shoji, H. & Miyakawa, T. Age-related behavioral changes from young to old age in male mice of a C57 <scp>BL</scp> /6J strain maintained under a genetic stability program. *Neuropsychopharmacol. Rep.* **39**, 100–118 (2019).
51. Kaufman, J. M. & Vermeulen, A. the decline of androgen levels in elderly men and its clinical and therapeutic implications. *Endocr. Rev.* **26**, 833–876 (2005).
52. Wu, F. C. W. et al. Hypothalamic-pituitary-testicular axis disruptions in older men are differentially linked to age and modifiable risk factors: The european male aging study. *J. Clin. Endocrinol. Metab.* **93**, 2737–2745 (2008).
53. McBride, J. A., Carson, C. C. & Coward, R. M. Testosterone deficiency in the aging male. *Ther. Adv. Urol.* **8**, 47–60 (2016).
54. Lessard-Beaudoin, M., Laroche, M., Demers, M.-J., Grenier, G. & Graham, R. K. Characterization of age-associated changes in peripheral organ and brain region weights in C57BL/6 mice. *Exp. Gerontol.* **63**, 27–34 (2015).
55. Yang, H. et al. the effects of aging on testicular volume and glucose metabolism: An investigation with ultrasonography and FDG-PET. *Mol. Imaging Biol.* **13**, 391–398 (2011).
56. Meyer, R. G. & Meyer-Ficca, M. L. Metabolism in male reproductive aging. *Adv. Geriatr. Med. Res.* **3**, e210005 (2021).
57. Barth, A. D. & Oko, R. J. *Abnormal morphology of bovine spermatozoa* (Iowa State University Press, 1989).
58. Rao, A. R., Bane, A. & Gustafsson, B. K. Changes in the morphology of spermatozoa during their passage through the genital tract in dairy bulls with normal and impaired spermat ogenesis. *Theriogenology* **14**, 1–12 (1980).
59. Harris, I. D., Fronczak, C., Roth, L. & Meacham, R. B. Fertility and the aging male. *Rev. Urol.* **13**, e184–e190 (2011).
60. Paoli, D. et al. Cytological and molecular aspects of the ageing sperm. *Hum. Reprod.* **34**, 218–227 (2019).
61. Kleshchev, M., Osadchuk, L. & Osadchuk, A. Age-related changes in sperm morphology and analysis of multiple sperm defects. *Front. Bioscie.-Scholar* **15**, 12 (2023).
62. Behdarvandian, P. et al. Sperm chromatin structure assay (SCSA®) and flow cytometry-assisted TUNEL assay provide a concordant assessment of sperm DNA fragmentation as a function of age in a large cohort of approximately 10,000 patients. *Basic Clin. Androl.* **33**, 33 (2023).
63. Zabihullah, Md. *et al.* The effect of age on semen quality among male partners of infertile couples: An observational study in a tertiary care center in Eastern India. *Cureus* **15** (2023).
64. de Losano, J. D. A. et al. Spermatic mitochondria: Role in oxidative homeostasis, sperm function and possible tools for their assessment. *Zygote* **26**, 251–260 (2018).
65. Leite, R. F. et al. Sperm function and oxidative status: Effect on fertility in Bos taurus and Bos indicus bulls when semen is used for fixed-time artificial insemination. *Anim. Reprod. Sci.* **237**, 106922 (2022).
66. Diao, R. et al. Decreased expression of cystic fibrosis transmembrane conductance regulator impairs sperm quality in aged men. *Reproduction* **146**, 637–645 (2013).
67. Ward, C. R. & Storey, B. T. Determination of the time course of capacitation in mouse spermatozoa using a chlortetracycline fluorescence assay. *Dev. Biol.* **104**, 287–296 (1984).
68. Sansegundo, E., Tourmente, M. & Roldan, E. R. S. Energy metabolism and hyperactivation of spermatozoa from three mouse species under capacitating conditions. *Cells* **11**, 220 (2022).
69. Kothari, S., Thompson, A., Agarwal, A. & du Plessis, S. S. Free radicals: Their beneficial and detrimental effects on sperm function. *Indian J. Exp. Biol.* **48**, 425–435 (2010).

70. Nagaki, C. A. P. et al. What is known so far about bull sperm protamination: A review. *Anim. Reprod.* **19**, e20210109 (2022).
71. Depa-Martynow, M., Kempisty, B., Jagodziński, P. P., Pawelczyk, L. & Jedrzejczak, P. Impact of protamine transcripts and their proteins on the quality and fertilization ability of sperm and the development of preimplantation embryos. *Reprod. Biol.* **12**, 57–72 (2012).
72. Gonzalez, M. B. *et al.* Reproductive Ageing: BGP-15 mitigates adverse impacts of aging on sperm quality fertility and offspring health in male mice. *Reproduction* **168** (2024).
73. Katz-Jaffe, M. G., Parks, J., McCallie, B. & Schoolcraft, W. B. Aging sperm negatively impacts in vivo and in vitro reproduction: a longitudinal murine study. *Fertil. Steril.* **100**, 262-268.e2 (2013).
74. Frattarelli, J. L., Miller, K. A., Miller, B. T., Elkind-Hirsch, K. & Scott, R. T. Male age negatively impacts embryo development and reproductive outcome in donor oocyte assisted reproductive technology cycles. *Fertil. Steril.* **90**, 97–103 (2008).
75. Wang, H. & Dey, S. K. Roadmap to embryo implantation: clues from mouse models. *Nat. Rev. Genet.* **7**, 185–199 (2006).
76. Nagy, A., Vintersten, K., Gertsenstein, M. & Behringer, R. R. *Manipulating the mouse embryo: A Laboratory manual*. (2003).
77. Alfarawati, S. et al. The relationship between blastocyst morphology, chromosomal abnormality, and embryo gender. *Fertil. Steril.* **95**, 520–524 (2011).
78. Liu, W.-M. et al. Sperm-borne microRNA-34c is required for the first cleavage division in mouse. *Proc. Natl. Acad. Sci.* **109**, 490–494 (2012).
79. Alves, M. B. R. et al. Sperm-borne miR-216b modulates cell proliferation during early embryo development via K-RAS. *Sci. Rep.* **9**, 10358 (2019).
80. Johnson, L. et al. K-ras is an essential gene in the mouse with partial functional overlap with N-ras. *Genes Dev.* **11**, 2468–2481 (1997).
81. Wigger, M. et al. Plasticity of the inner cell mass in mouse blastocyst is restricted by the activity of FGF/MAPK pathway. *Sci. Rep.* **7**, 15136 (2017).
82. Avilion, A. A. et al. Multipotent cell lineages in early mouse development depend on SOX2 function. *Genes Dev.* **17**, 126–140 (2003).
83. Keramari, M. et al. Sox2 Is essential for formation of trophectoderm in the preimplantation embryo. *PLoS ONE* **5**, e13952 (2010).
84. Wicklow, E. et al. HIPPO pathway members restrict SOX2 to the inner cell mass where it promotes ICM fates in the mouse blastocyst. *PLoS Genet.* **10**, e1004618 (2014).
85. Denomme, M. M., Haywood, M. E., Parks, J. C., Schoolcraft, W. B. & Katz-Jaffe, M. G. The inherited methylome landscape is directly altered with paternal aging and associated with offspring neurodevelopmental disorders. *Aging Cell* **19**, e13178 (2020).
86. Licciardi, F., McCaffrey, C., Oh, C., Schmidt-Sarosi, C. & McCulloh, D. H. Birth weight is associated with inner cell mass grade of blastocysts. *Fertil. Steril.* **103**, 382-387.e2 (2015).
87. Shi, S., Zhao, B., Hu, Z. & Shi, Q. The impact of blastocyst grade on singleton birth weight in fresh IVF-ET cycles in ART: A retrospective study. *BMC Pregnancy Childbirth* **24**, 588 (2024).
88. Du Sert, N. P. et al. Reporting animal research: Explanation and elaboration for the ARRIVE guidelines 2.0. *PLoS Boil.* **18**(7), e3000411 (2020).
89. Concea. Diretriz da Prática de Eutanásia do Concea - Resolução Normativa nº 37 - de 27/01/18. https://antigo.mctic.gov.br/mctic/opencms/legislacao/outros_atos/resolucoes/Resolucao_CONCEA_n_37_de_15022018.html (2018).
90. de Garcia-GomesSouza. Aranha, M. et al. Behavioral and neurochemical characterization of the spontaneous mutation tremor, a new mouse model of audiogenic seizures. *Epilepsy & Behav.* **105**, 106945 (2020).
91. Goissis, M. D. & Cibelli, J. B. Functional characterization of CDX2 during bovine preimplantation development in vitro. *Mol. Reprod. Dev.* **81**, 962–970 (2014).
92. Wyrobek, A. J. & Bruce, W. R. Chemical induction of sperm abnormalities in mice. *Proc. Natl. Acad. Sci. U S A* **72**, 4425–4429 (1975).
93. Bruner-Tran, K. L. et al. Developmental exposure of mice to dioxin promotes transgenerational testicular inflammation and an increased risk of preterm birth in unexposed mating partners. *PLoS ONE* **9**, e105084 (2014).
94. Musa, N. H. C., Zain, H. H. M., Ibrahim, H. & Jamil, N. N. M. Evaluation of acute and sub-acute oral toxicity effect of *Aquilaria malaccensis* leaves aqueous extract in male ICR mice. *Nat. Prod. Sci.* **25**, 157 (2019).
95. Ghosh, S. & Mukherjee, S. Testicular germ cell apoptosis and sperm defects in mice upon long-term high fat diet feeding. *J. Cell Physiol.* **233**, 6896–6909 (2018).
96. Goovaerts, I. G. F. et al. Evaluation of epididymal semen quality using the hamilton-thorne analyser indicates variation between the two caudae epididymides of the same bull. *Theriogenology* **66**, 323–330 (2006).
97. Castro, L. S. et al. Effect of bovine sperm chromatin integrity evaluated using three different methods on in vitro fertility. *Theriogenology* **107**, 142–148 (2018).
98. de Castro, L. S. et al. Sperm oxidative stress is detrimental to embryo development: A dose-dependent study model and a new and more sensitive oxidative status evaluation. *Oxid Med Cell Longev* **2016**, 8213071 (2016).
99. Barbosa-Moyano, H., Zacariotti, R. L. & de Oliveira, C. A. Validation of enzyme immunoassays for quantifying sex steroid hormones in tropical screech owls (Megascops choliba). *Gen. Comp. Endocrinol* **345**, 114386 (2024).

Acknowledgements

This work was supported by the Sao Paulo Research Foundation (FAPESP) under grant 21/11747-6 and 18/18297-3; Coordination for Improvement of Higher Education Personnel (CAPES) under grant 88887.658490/2021-00. The authors thank Mr. Waldir Caldeira, MSc. and the Center for Image Acquisition and Microscopy at the Institute of Biosciences of the University of São Paulo (CAIMI-IB-USP) for assistance with imaging using the confocal microscope.

Author contributions

T.R.S.H., C.M.M., L.A.S. and M.E.O.A.A. designed the experimental study. L.A.S., T.R.S.H. and C.M.M. collected and analyzed the samples. A.M.A. and M.N. performed the CASA evaluation. H.B.M. and L.A.S. conducted and analyzed the serum testosterone levels. L.A.S., M.S.A.G.G., and C.C.M. performed the behavioral analyses. L.A.S. conducted the immunofluorescence analysis and designed the images and tables. T.R.S.H. and M.N. conducted the statistical analyses. L.A.S., T.R.S.H., C.M.M., M.D.G., and M.N. drafted the manuscript. M.E.O.A.A. and J.A.V. provided financial support and completed the critical revision and approval of the manuscript.

Funding

Coordenação de Aperfeiçoamento de Pessoal de Nível Superior, 88887.658490/2021-00, 88887.658490/2021-00, Fundação de Amparo à Pesquisa do Estado de São Paulo, 18/18297-3, 18/18297-3, Conselho Nacional de Desenvolvimento Científico e Tecnológico, 310061/2022-9, Fundação de Amparo à Pesquisa do Estado de São

Paulo, Brazil, 21/11747-6.

Declarations

Competing interests
The authors declare no competing interests.

Additional information
Supplementary Information The online version contains supplementary material available at https://doi.org/10.1038/s41598-025-08743-3.

Correspondence and requests for materials should be addressed to M.E.O.D.A.

Reprints and permissions information is available at www.nature.com/reprints.

Publisher's note Springer Nature remains neutral with regard to jurisdictional claims in published maps and institutional affiliations.

Open Access This article is licensed under a Creative Commons Attribution-NonCommercial-NoDerivatives 4.0 International License, which permits any non-commercial use, sharing, distribution and reproduction in any medium or format, as long as you give appropriate credit to the original author(s) and the source, provide a link to the Creative Commons licence, and indicate if you modified the licensed material. You do not have permission under this licence to share adapted material derived from this article or parts of it. The images or other third party material in this article are included in the article's Creative Commons licence, unless indicated otherwise in a credit line to the material. If material is not included in the article's Creative Commons licence and your intended use is not permitted by statutory regulation or exceeds the permitted use, you will need to obtain permission directly from the copyright holder. To view a copy of this licence, visit http://creativecommons.org/licenses/by-nc-nd/4.0/.

© The Author(s) 2025